Inverting for emissions of carbon monoxide from Asia using aircraft observations over the western Pacific

Paul I. Palmer, Daniel J. Jacob, Dylan B. A. Jones, Colette L. Heald, Robert M. Yantosca,

Jennifer A. Logan

Division of Engineering and Applied Sciences, Harvard University, Cambridge MA

Glen W. Sachse

NASA Langley Research Center, VA

David. G. Streets

Argonne National Laboratory, Argonne IL

Short title: INVERSION OF ASIAN CO EMISSIONS DURING TRACE-P

Abstract. We use aircraft observations of continental outflow over the western Pacific from the TRACE-P mission (March-April, 2001), in combination with an inverse model, to improve emission estimates of carbon monoxide (CO) from Asia. We use as *a priori* a customised bottom-up Asian emission inventory for the TRACE-P period and apply an optimal estimation inverse method to calculate *a posteriori* emissions that are consistent with both the observed CO distribution, the bottom-up inventory, and their respective errors. The global GEOS-CHEM chemical transport model (CTM) is the forward model in the inverse method. We describe an innovative method to quantify model transport error from the relative error statistics between the aircraft observations of CO and the forward model results with *a priori* emissions. We assume that the mean relative error is determined by errors in *a priori* emissions, while the residual variance in the relative error is due to the model transport. The model transport error is found to be typically 20-30%; additional contributions to the error budget in the inverse analysis include the representativeness error (typically 5%), and measurement noise ($<$1%). Analysis of averaging kernels suggests that the inverse model can usefully constrain six sources: Chinese fuel consumption, Chinese biomass burning, combined total emissions from Korea and Japan, total emissions from Southeast Asia, total emissions from India, and the ensemble of all other sources. The principal result of the inversion is a 30% increase in anthropogenic emission from China (to 142 Tg CO yr^{-1}) relative to the *a priori*; this value is still much lower than had been derived in previous inversions using the sparse network of surface observations. *A posteriori* emissions of biomass burning in Southeast Asia and India are much lower than assumed *a priori*.

1. Introduction

Understanding and predicting the atmospheric distribution of a chemical species requires information on the emissions of that species and of its precursors. The bottom-up approach to compiling emission inventories generally relies on emission factors for individual processes, extrapolated in space and time using socioeconomic or energy data. Top-down constraints from atmospheric concentration measurements, interpreted with a chemical tracer model (CTM), can be used to improve the bottom-up estimates through an optimal estimation methodology (inverse model). Almost all inverse modeling studies of emissions so far have used atmospheric concentrations measured from networks of surface sites; however, these sites are often not well situated to provide constraints on emissions. We present here the first application of inverse modeling to observations from an aircraft mission targeted at sampling continental outflow. As we will show, the high density of aircraft observations over a range of outflow pathways provides considerable information for inverse modeling, and also allows us to quantify CTM transport errors for use in the inverse model. Our detailed specification of these errors represents a major advance over previous inverse model studies.

We apply the inverse model approach to aircraft observations of carbon monoxide (CO) taken during the NASA Transport And Chemical Evolution over the Pacific (TRACE-P) mission in March-April 2001 [*Jacob et al.*, 2002]. The TRACE-P mission used two aircraft (DC-8 and P-3B), based in Hong Kong and Tokyo, to sample Asian chemical outflow along the Pacific rim (Plate 1). Carbon monoxide is a general product of incomplete combustion, and has an atmospheric lifetime of a few months against oxidation by OH, its main sink.

Plate 1

Asian sources of CO during TRACE-P included anthropogenic emissions from fossil fuel and biofuel consumption, as well as seasonal biomass burning in Southeast Asia [*Streets et al.*, 2002; *Heald et al.*, 2002b]. The major meteorological processes leading to outflow of anthropogenic Asian pollution during TRACE-P included warm conveyor belts (WCBs) ahead of southeastward-moving cold fronts, and transport in the boundary layer behind these fronts [*Liu et al.*, 2002]. Outflow of biomass burning effluents from Southeast Asia took place by deep convection, and by WCBs, the latter process leading to mixing with the anthropogenic outflow [*Ma et al.*, 2002; *Tang et al.*, 2002]. The lifetime of CO is long enough that long-range transport from European and North American sources, as well as oxidation of methane and biogenic non-methane volatile organic compounds (NMVOCs), also contributes to Asian outflow; but these contributions are mainly to background CO and did not produce detectable enhancements in the TRACE-P observations [*Liu et al.*, 2002].

Our inversion analysis uses the TRACE-P aircraft observations, together with *a priori* information on Asian emissions from customised bottom-up inventories produced for the TRACE-P period [*Streets et al.*, 2002; *Heald et al.*, 2002b], to obtain optimised *a posteriori* estimates of CO emissions from different source regions in Asia. The inverse model approach has been used previously in three studies investigating the emissions of CO [*Bergamaschi et al.*, 2000; *Kasibhatla et al.*, 2002; *Pétron et al.*, 2002]. These studies all used the global measurements of CO from the NOAA/CMDL network [*Novelli et al.*, 1998] as top-down constraints. *Bergamaschi et al.* [2000] found that their bottom-up emission inventories were too low and attributed the cause either to anthropogenic emissions or to the source of CO from oxidation of biogenic terpenes. *Kasibhatla et al.* [2002] and *Pétron et al.* [2002] used

a geographically disaggregated approach to identify emissions from specific regions. In particular, *Kasibhatla et al.* [2002] found that their *a priori* emissions from Asia were too low, and reconciled this with the rapid industrialisation of the region in recent years. One major disadvantage to using NOAA/CMDL stations for inverse modeling of continental source emissions is that they are positioned purposely to measure the remote troposphere; and consequently concentrations measured at these sites tend to have complex source signatures.

In the next section we briefly describe the GEOS-CHEM CTM used here to simulate CO during TRACE-P, and present a comparison between the modeled and measured concentrations of CO. Section 3 describes the inverse model and explores the potential of TRACE-P measurements to constrain emission estimates from particular geographical regions. Section 4 presents the inverse model analysis of the TRACE-P data, and investigates the sensitivity of results to different assumptions. Section 5 places the results in the context of previous work. We conclude the paper in section 6.

2. GEOS-CHEM Model Simulation of CO During TRACE-P

2.1. Model Description

The GEOS-CHEM global 3-D model of tropospheric chemistry [*Bey et al.*, 2001a] is used here to relate sources of CO to atmospheric concentrations, and constitutes the forward model in the inverse analysis (section 3). A recent application of GEOS-CHEM to the simulation of CO, including evaluation with the ensemble of NOAA/CMDL observations, is presented by *Duncan et al.* [2002a]. The model version used here (v4.33, http://www-

as.harvard.edu/chemistry/trop/geos/index.html) has a horizontal resolution of 2° latitude $\times 2.5^\circ$ longitude, and has 48 vertical levels ranging from the surface to the mesosphere, 20 of which are below 12 km. The model is driven by assimilated meteorology from the Goddard Earth Observing System (GEOS) of the NASA Data Assimilation Office. The 3-D meteorological data are updated every six hours; mixing depths and surface fields are updated every three hours.

Gridded CO emission inventories for fossil fuel, biofuel, and biomass burning in East Asia during the TRACE-P period [*Streets et al.*, 2002; *Heald et al.*, 2002b] are used as *a priori* by the model. The *Streets et al.* [2002] inventory describes anthropogenic fossil fuel and biofuel emissions for the year 2000. Fossil fuel emissions are from residential coal (used for cooking and heating), transportation, and industry. Daily, weekly and seasonal variability in fossil fuel emissions reflects changes largely in transportation. We account only for daily and weekly variability; seasonal variation of fossil fuel emissions from transportation represents only a small fraction of total CO emissions from countries within Asia [*Streets et al.*, 2002]. The biofuel inventory of *Streets et al.* [2002] includes sources from fuel wood, agricultural residues, and dung. The seasonal variation of biofuels, associated mainly with domestic heating, is presented by *Streets et al.* [2002] and represents only a few percent of the total emissions of CO from Asia. During TRACE-P biofuel emissions were found to be approximately at their annual mean value [*Streets et al.*, 2002], with emissions during April 10% lower than those during March due to the exiting of the domestic heating season. This seasonality is not considered in our model. *Streets et al.* [2002] provide detailed error estimates associated with their national emissions from Asia, representing important information for the

inverse model analysis. Fossil fuel and biofuel emissions for the rest of the world are taken here from *Duncan et al.* [2002a] and *Yevich and Logan* [2002], respectively.

We use daily biomass burning CO emissions for the TRACE-P period from *Heald et al.* [2002b]. This inventory uses firecount data from the AVHRR satellite instrument [*Stroppiana et al.*, 2000] to constrain daily variability. It applies this variability to the biomass burning emission inventory of CO from *Duncan et al.* [2002b], which includes interannual and seasonal variability derived from TOMS, ATSR, and AVHRR satellite observations. Global biomass burning emissions during TRACE-P were mainly from Southeast Asia and India, and were approximately the same as the climatological average for February−April [*Heald et al.*, 2002b].

In addition to direct emissions of CO there is a large chemical source from the oxidation of methane and NMVOCs which is treated here following the approach of *Duncan et al.* [2002a]. Anthropogenic and biomass burning NMVOCs are in general co-emitted with CO; following *Duncan et al.* [2002a] we model them here as direct sources of CO and correspondingly increase the primary emissions of CO by 20% (fossil fuel) and 10% (biofuel and biomass burning). Additional sources of CO in the model include methane (850 Tg CO/yr), and biogenic NMVOCs with contributions from isoprene (175 Tg CO/yr), methanol (85 Tg CO/yr), monoterpenes (70 Tg CO/yr), and acetone(25 Tg CO/yr). Details of these sources can be found in *Duncan et al.* [2002a].

The main sink for CO is oxidation by OH. We use prescribed monthly mean OH concentration fields calculated from a full-chemistry simulation conducted with GEOS-CHEM v4.33. The corresponding lifetime of methylchloroform (CH_3CCl_3), a proxy for

the global mean OH concentration, is 6.3 years; this is consistent with the best estimate of $5.99^{+0.95}_{-0.71}$ years by *Prinn et al.* [2001] from CH_3CCl_3 measurements. A detailed discussion of the factors affecting the CH_3CCl_3 lifetime in GEOS-CHEM is presented by *Martin et al.* [2002]. Although adjustment of CO sources in the inverse model analysis should modify OH, the effect is inconsequential for inverting Asian sources using the TRACE-P observations, which are only a few days downwind of the sources. This assumption of fixed OH linearises the inverse problem [*Kasibhatla et al.*, 2002]. Jacobian matrices for the inversion, relating individual sources of CO to the resulting atmospheric concentrations, can then be readily generated with a 'tagged' CO simulation in which total CO is linearly decomposed into contributions from sources in different geographic regions and of different types (Figure 1; Table 1).

Figure 1

Table 1

A number of previous GEOS-CHEM model studies have evaluated the simulation of CO with surface and aircraft observations in different regions of the world [*Bey et al.*, 2001ab; *Fiore et al.*, 2002; *Li. et al.*, 2002; *Martin et al.*, 2002; *Duncan et al.*, 2002a; *Kasibhatla et al.*, 2002]. These studies used different versions of GEOS-CHEM, with different CO sources and OH concentrations, so that results are not strictly comparable. The global underestimate of CO reported in the original version of GEOS-CHEM [*Bey et al.*, 2001a] has since been corrected by better accounting of NMVOC precursors and of various factors acting to reduce OH [*Martin et al.*, 2002; *Duncan et al.*, 2002a]. The most recent global evaluation [*Duncan et al.*, 2002a] indicates no bias in the simulation of the CO background, and this appears to hold also for v4.33 used here [*Heald et al.*, 2002b]. However, both *Duncan et al.* [2002a] and

Heald et al. [2002b] used an anthropogenic Chinese source of CO that is 20% higher than the *Streets et al.* [2002] inventory used here.

2.2. Evaluation of model with *a priori* sources

Before proceeding with the inversion we first examine the ability of the *a priori* sources, as described in section 2.1, to simulate the TRACE-P measurements of CO. Spectroscopic measurements of CO were taken during TRACE-P using the Differential Absorption CO Measurement (DACOM) [*Sachse et al.*, 1987]. CO was measured at a frequency of 1 Hz with an estimated 1-second precision of 1%. We use here the 1-minute average data, and further average it over the GEOS-CHEM $2\times2.5^\circ$ grid along the flight tracks for the purpose of model evaluation.

The GEOS-CHEM simulations of CO and tagged CO tracers were intialised in January 2000 and conducted for 16 months (through April 2001). The 14-month simulation before the start of TRACE-P effectively removes the influence from initial conditions. We sample the model fields along TRACE-P flight tracks, and compare to the observations averaged over the $2\times2.5^\circ$ model grid. We remove stratospherically influenced air as diagnosed by $O_3 > 100$ ppb, and verified that this criterion does not remove any pollution plumes (O_3 was occasionally above 100 ppb in Chinese urban plumes, but not when averaged over the $2\times2.5^\circ$ grid). We also ignore data east of 150°E, which are mainly from transit flights (Plate 1).

A general statistical comparison of model results with observations is shown in Figure 2. The model is on average 23 ppb too low; this discrepancy is driven by the high tail of the distribution (CO>200 ppb), representing strong outflow from Asia. The frequency distribution

Figure 2

of differences between model and observations shows an approximate Gaussian distribution with a 13 ppb negative bias in the median. Major pollution plumes in the observations (CO>500 ppb) are not well captured by the model.

A more detailed evaluation of the model with observations is shown in Plate 2 by the latitudinal gradients at different altitudes from 0 to 12 km. The model has a negative bias in the boundary layer which increases with latitude, reaching 80 ppb (30% of the mean total CO) between 30−40°N. We attribute this negative bias to an underestimate of Chinese anthropogenic emissions, as discussed below. Above the boundary layer the negative model bias is less, and largely disappears south of 30°N or above 6 km. The concentration of CO in the free troposphere is relatively more sensitive to biomass burning and to sources outside of Asia [*Liu et al.*, 2002].

Plate 2

3. Inverse Model

3.1. Description

Measured concentrations of CO (assembled in measurement vector $\mathbf{y}$), are related to the sources of CO (assembled in a state vector $\mathbf{x}$) by the following relation:

$$\mathbf{y} = \mathbf{K}\mathbf{x} + \boldsymbol{\epsilon}. \tag{1}$$

The state vector $\mathbf{x}$ as defined here comprises annual source estimates from different geopolitical regions and from different CO source types; its composition will be discussed in section 3.3. The measurement vector $\mathbf{y}$ comprises the TRACE-P CO data averaged along

the flight tracks over the model grid. The Jacobian matrix $\mathbf{K}$ describes the forward model and is constant under our linear assumption. The error vector $\boldsymbol{\epsilon}$ includes contributions from measurement noise, sub-grid variability of observations, and errors in model parameters (transport, chemistry, sub-regional emission patterns). The ensemble characteristics of these errors are described by the measurement error covariance $\mathbf{S}_{\Sigma}$, representing a sum of the covariance matrices from individual sources of error.

An inverse model describes the mathematical mapping from the measurement vector to the state vector. Here, the inverse model describes the best estimate of sources of CO that is consistent with both the aircraft observations of CO concentrations during TRACE-P and the *a priori* sources of CO, given their respective uncertainties. The fundamental idea of an optimal estimation inverse method is to minimise a cost function $\mathbf{J}(\mathbf{x})$ (that is, to solve $\nabla_{\mathbf{x}}\mathbf{J}(\mathbf{x}) = 0$). We use a standard least-squares formulation for $\mathbf{J}(\mathbf{x})$:

$$\mathbf{J}(\mathbf{x}) = (\mathbf{y} - \mathbf{K}\mathbf{x})^{\mathrm{T}}\mathbf{S}_{\Sigma}^{-1}(\mathbf{y} - \mathbf{K}\mathbf{x}) + (\mathbf{x} - \mathbf{x}_a)^{\mathrm{T}}\mathbf{S}_a^{-1}(\mathbf{x} - \mathbf{x}_a), \tag{2}$$

where $\mathbf{x}_a$ is the *a priori* value of the state vector (comprised of the *a priori* sources), $\mathbf{S}_a$ is the estimated error covariance matrix for $\mathbf{x}_a$, and all other variables are as defined previously. Solution to $\nabla_{\mathbf{x}}\mathbf{J}(\mathbf{x}) = 0$ yields

$$\hat{\mathbf{x}} = \mathbf{x}_a + (\mathbf{K}^{\mathrm{T}}\mathbf{S}_{\Sigma}^{-1}\mathbf{K} + \mathbf{S}_a^{-1})^{-1}\mathbf{K}^{\mathrm{T}}\mathbf{S}_{\Sigma}^{-1}(\mathbf{y} - \mathbf{K}\mathbf{x}_a) \tag{3}$$

$$\hat{\mathbf{S}} = (\mathbf{K}^{\mathrm{T}}\mathbf{S}_{\Sigma}^{-1}\mathbf{K} + \mathbf{S}_a^{-1})^{-1}, \tag{4}$$

where $\hat{\mathbf{x}}$ is the optimised *a posteriori* state vector and $\hat{\mathbf{S}}$ is the *a posteriori* error covariance matrix, describing the error on $\hat{\mathbf{x}}$. The value of the cost function before, during, and after all the observations have been ingested provides a useful indication of the quality of the inversion. In a successful inversion, $\mathbf{J}(\mathbf{x})$ should be of the same order as the number of observations. A value of $\mathbf{J}(\mathbf{x})$ that is too large signals that one or more contributions comprising $\mathbf{S}_\Sigma$ may be underestimated or that the prior constraint is too tight; alternatively if $\mathbf{J}(\mathbf{x})$ is too small one or more contributions comprising $\mathbf{S}_\Sigma$ may be overestimated or the prior constraint may be too loose.

3.2. Error Specification

The Asian emission inventory of *Streets et al.* [2002], used here to define the *a priori* state vector $\mathbf{x}_a$, includes uncertainty estimates for individual countries and processes derived by propagation of errors in the bottom-up approach. These uncertainties are listed in Table 1. Additionally we assign source uncertainties of 30% for North America and Europe and 50% for the rest of the world; TRACE-P was not designed to provide information on these regions so accurate specification of errors is not essential. We assign the source from biomass burning an uncertainty of 50%. The chemical source from oxidation of methane and biogenic NMVOCs is defined largely by methane, and we assign it an uncertainty of 25% based on constraints on global OH from observations of CH_3CCl_3 [*Prather and Enhalt*, 2001]. The sensitivity of the *a posteriori* solution to the assumed emission uncertainties in the inverse model will be assessed in section 4.

The total measurement error $\mathbf{S}_\Sigma$ includes contributions from observation noise,

representativeness errors, and errors in the forward model. Estimating errors due to the model is non-trivial. We do so here by computing the statistics of the relative difference between the aircraft observations and the model, $(\mathbf{K}\mathbf{x}_a - \mathbf{y})/\mathbf{y}$, as a function of altitude and for two latitude ranges (Figure 3). We assume that the mean model bias, as diagnosed by the mean relative difference, is due to errors in the *a priori* sources, and that the variance about this mean value represents errors due to the model. *Bey et al.* [2002] showed that the GEOS-CHEM simulation of transport during TRACE-P was unbiased, supporting our assumption, and an intercomparison of CTM simulations of CO during the TRACE-P period [*Kiley et al.*, 2002] also shows no evident GEOS-CHEM transport bias. By subtracting the mean bias for each altitude and latitude range in Figure 3 we are left with the residual relative error (RRE). Then for each individual observation y_i we calculate an absolute model error as RRE$\times y_i$. We assume no error covariance between observations. Typical values for the RRE are between 0.2 and 0.3, as can be seen from Figure 3. The RREs calculated from the simulation with *a priori* sources show higher values in the free troposphere, but this difference disappears in the simulation with *a posteriori* sources, discussed below.

Figure 3

Values of the mean bias as shown in Figure 3 are consistent with those reported in Figure 2. The TRACE-P domain (Plate 1) can be split into two distinct regions, characterized by differences in airmasses sampled [*Blake et al.*, 2002]. North of 30°N, airmasses were heavily influenced by fossil fuel and biofuel emissions from China, Korea and Japan; south of 30°N and in the free troposphere airmasses were influenced also by biomass burning. Mean bias statistics for both regions show an underestimate of emissions in the boundary layer. In the free troposphere, there is still an underestimate above 30°N but an overestimate at lower

latitudes. These mean bias statistics suggest that *a priori* anthropogenic emissions are too high, while biomass burning emissions are too low.

Our method of quantifying model transport error is a major advance over previous inverse model studies which have estimated the total measurement error by calculating the standard deviation of the discrepancy between model and measured monthly mean values in the surface data used for the inversions (e.g., *Bousquet et al.* [1999], *Kasibhatla et al.* [2002]). Our method can be used iteratively to improve the estimate for model errors. To illustrate this we re-calculated values of RRE using the *a posteriori* CO sources (to be presented in section 4). We find that the *a posteriori* sources, although they reduce greatly the bias between simulated and observed concentrations, yield values of RRE that are comparable with those calculated using *a priori* emissions. This supports our assumption that the mean bias is largely due to errors in the emissions and the variability is due to errors in the transport.

Additional errors contributing to $\mathbf{S}_{\sum}$ include measurement noise ($<$1% of the concentration) and representativeness error, describing the mismatch between the model and observations due to sub-grid scale variability. We quantify the representiveness error by examining statistics of the sub-grid variability in the observations over the $2\times2.5^{\circ}$ GEOS-CHEM model grid. We compute this error for each sampled model grid square and find that it is typically 5-10%. We thus find in our error analysis that model error represents typically 73% (mean=38 ppb) of the total measurement error budget and is therefore the most important to quantify; representativeness error accounts for approximately 25% (mean=14 ppb); and instrument noise account for the remaining 2% (mean=2 ppb).

3.3. Selection of State Vector

The ability of the observing system to determine different elements of the state vector, taking into account the assigned measurement and *a priori* state uncertainties, can be tested by inspecting the matrix of averaging kernels $\mathbf{A} = \mathbf{I} - \hat{\mathbf{S}}\mathbf{S}_a^{-1}$, where $\mathbf{I}$ is the identity matrix [*Rodgers*, 1976], and $\hat{\mathbf{S}}$ is computed from equation 4. Averaging kernels peaked at their own state vector element denote a well constrained source. Starting from the ensemble of source regions and processes in Table 1, we used averaging kernels to determine which sources or aggregation of sources could be constrained independently with the TRACE-P data. We find that fossil fuel and biofuel emissions within a given country are too co-located to be retrieved independently, and such is the case also for biomass burning except for China. We must also aggregate emissions from Japan and Korea, as TRACE-P does not provide independent information on the two (Japanese outflow sampled in TRACE-P had generally passed previously over Korea [*Palmer et al.*, 2003]). We thus define a six-component state vector (CHBFFF, KRJP, SEA, IN, CHBB, RW) for which the averaging kernels are shown in Plate 3. Even with this aggregated state vector there is poor definition of the combined Korea and Japan source, reflecting the relatively small uncertainties assigned by *Streets et al.* [2002] for *a priori* emissions from these countries (Table 1). We also find that the Chinese biomass burning source is strongly correlated with the non-Asian source of CO (rest of the world); both of these sources affect mostly the free troposphere in the TRACE-P observations.

Plate 3

4. Results

We apply the optimal inverse model described in the previous section to the TRACE-P data. We use a χ^2 quality control to remove outliers (4% of the data), leaving 1825 observations. Results shown in Plate 4 indicate that the *a priori* anthropogenic emissions from China are 30% too low, while emission estimates defined largely by biomass burning (SEA and IN) are too high. The inversion returns negative emissions for India, an unphysical result which will be discussed below. The increase in Chinese anthropogenic emissions is driven by the model underestimate in the boundary layer (Plate 2 and 3), while the decrease in biomass burning derives from the model overestimate in the free troposphere (Plate 2 and Figure 3). There is also a 20% increase in the source from the rest of the world which represents effectively a correction to the background. The cost function (equation 2) computed using *a priori* emissions is 2120, a value larger than the number of observations (n=1909), which after the measurements have been ingested, is reduced by 30% to 1497, suggesting an overall improvement in the prescribed emission sources.

Plate 4

We can test the utility of the inverse model by using the *a posteriori* emissions with the tagged tracers in the forward model to simulate TRACE-P observations. In this simulation, the contribution of Indian sources of CO along the TRACE-P flight tracks is effectively zero. In general *a posteriori* emissions improve the comparison with observations (Figure 2). The median value of the difference between model and observed CO decreases from -14 ppb to -4 ppb, while the mean bias is reduced by 30%. The lesser improvement in the mean reflects the difficulty in reproducing the high tails of the observed frequency distribution. The

frequency distribution of the differences is noticeably tighter. Plate 2 shows that in general the *a posteriori* emissions simulate the observed latitudinal variability of CO better than the *a priori* emissions, significantly reducing the large discrepancies in the boundary layer and elsewhere.

The inverse model approach is sensitive to uncertainties assumed for the measurements ($\mathbf{S}_\Sigma$) and the *a priori* emissions ($\mathbf{S}_a$) (equation 4). Model error largely defines the measurement error $\mathbf{S}_\Sigma$ (section 3). We find that doubling and halving the uncertainty of emission estimates and model error leads to results not statistically different from the best estimate, i.e., all results$\pm 1\sigma$ values are consistent, suggesting that our best estimate of *a posteriori* sources is robust (Plate 5). The only notable exception is India whose results change significantly when the source emission uncertainty is halved or when the model error is doubled. *A priori* biomass burning emissions from India are assigned a large uncertainty (Table 1). It is likely that our statistical representation of the model transport error based on the RRE underestimates the actual error in modeling the transport of Indian outflow to the TRACE-P region. Indian influence in the model along TRACE-P flight tracks is mainly from a few flights, and reflects biomass burning effluents lifted by convection to the free troposphere and then advected in the westerlies. Convective events in GEOS-CHEM (and other global or mesoscale CTMs) are parameterised as sub-grid processes and difficult to simulate deterministically. Indeed, the *Kiley et al.* [2002] intercomparison of TRACE-P simulations of CO shows that agreement with observations was worst during convective events diagnosed by satellite infrared imagery.

Plate 5

5. Comparison with Previous Work

Kiley et al. [2002] presented an intercomparison of TRACE-P CO simulations from seven different CTMs using the *Streets et al.* [2002] emission inventory for Asia. All models found an underestimate of CO in the boundary layer, consistent with the results presented here and which we attribute to a 30% underestimate of anthropogenic Chinese emissions (*a posteriori* emission value = 142 Tg CO/yr). *Carmichael et al.* [2002] also investigated this underestimate of Chinese CO with a regional CTM and attributed it to an underestimate in emissions from the domestic combustion sector, in particular from residential coal burning. They tentatively suggest that a factor of 3-5 increase in the *Streets et al.* [2002] inventory for that sector would be required to reconcile model results with the observed concentrations. Such an increase would correspond to Chinese anthropogenic emissions of 169−228 Tg CO/yr, a value 20−60% greater than the value presented here. *Carmichael et al.* [2002] focussed on data from just a few flights. Our inverse model approach, by using the ensemble of flight data, may be more suitable for national extrapolation.

Our *a posteriori* biomass burning emissions are considerably lower than the *a priori* values, a result largely driven by the measurements in the free troposphere (Plate 2). This result is qualitatively consistent with CO column data from the MOPITT satellite instrument, which imply much lower biomass burning emissions of CO in Southeast Asia and Northeast India than used here as *a priori* [*Heald et al.,* 2002a]. Correlations of CO with HCN in the TRACE-P data, with HCN taken as a tracer of biomass burning, do not imply an underestimate of biomass burning CO emissions [*Li et al.,* 2002; *Heald et al.,* 2002b].

Anthropogenic Chinese sources of HCN may complicate this interpretation [*Singh et al.*, 2002]. A multi-species inversion would then be needed to exploit such correlations between CO and other species measured in TRACE-P.

Specific investigation of biomass burning influences in the TRACE-P data was conducted by *Carmichael et al.* [2002] and *Tang et al.* [2002] using their regional CTM with Asian biomass burning emissions (67 Tg CO/yr) that are a factor of two smaller than our *a priori* values. *Carmichael et al.* [2002] constructed spatial maps of emitted CO concentrations using back-trajectories from observed and simulated TRACE-P CO concentrations. They found, in particular, large differences over biomass burning regions of Southeast Asia and Northeast India. *Tang et al.* [2002] used their CTM to identify nine flights during TRACE-P that were particularly impacted by biomass burning emissions from Southeast Asia. We analysed these flights using our *a priori* and *a posteriori* emissions and found no significant bias in the simulations.

Kasibhatla et al. [2002] and *Pétron et al.* [2002] previously used CO observations from the CMDL network [*Novelli et al.*, 1998] to determine Asian sources of CO. Both studies found that their *a priori* Asian emissions [*Olivier et al.*, 1996] were too low. *Kasibhatla et al.* [2002] showed that a 50% increase in Asian fuel consumption (to 350-380 Tg CO/yr) and a 100% increase in Asian biomass burning emissions (to 110-130 Tg CO/yr) were required to reconcile the CMDL concentration data from 1994; while *Pétron et al.* [2002] used data averaged between 1990-1996 and required a factor of two increase in Asian anthropogenic emissions (to 548 Tg CO/yr) and a 25% increase in emissions from biomass burning. Our *a posteriori* anthropogenic source of CO from Asia (Table 1) is less than that derived in these

two studies, and our *a posteriori* biomass burning source of CO is much lower. In general, differences in magnitude of *a posteriori* emissions between those reported here and those reported by *Kasibhatla et al.* [2002] and *Pétron et al.* [2002] are likely due to the type of data used to determine continental source emissions. In particular, *Kasibhatla et al.* [2002] and *Pétron et al.* [2002] derived emission estimates using the sparse network of NOAA/CMDL surface observations that are not intended to sample continental air masses. Consequently, different sources of CO that contribute to these data are difficult to interpret. Here, we report emission estimates that use high density aircraft observations of continental outflow directly downwind of source emissions which are ideal for determining continental sources. In particular, *Pétron et al.* [2002] use a biomass burning inventory that overestimates the source of CO from agricultural waste burning [*Kasibhatla et al.*, 2002], and because they assign uncertainties using a percentage of the emissions, the uncertainty of the Asian state vector element is overestimated. Consequently Asian emissions can be adjusted more easily to improve the fit to observations than other emission sources, leading to an unphysically large emission estimate for Asia. The source of CO from the rest of the world, including the source from chemical oxidation, is comparable between the inverse model studies: 2340 Tg CO yr^{-1} [*Pétron et al.*, 2002], 2240 Tg CO yr^{-1} [*Kasibhatla et al.*, 2002], and 2240 Tg CO yr^{-1} for the work shown here.

6. Conclusions

We used aircraft observations of Asian outflow from the TRACE-P mission to improve estimates of CO emissions from Asia using an optimal estimation inverse method. This is the

first time than an inverse model has been applied to infer emissions from a large geopolitical source region using aircraft observations. We showed that the high density of coverage from an aircraft mission allows quantification of model transport error, a notorious difficulty in inverse modeling.

We used the GEOS-CHEM CTM, driven by customised *a priori* bottom-up emission inventories for Asia [*Streets et al.*, 2002; *Heald et al.*, 2002b] as a forward model to simulate the aircraft observations. The *Streets et al.* [2002] inventory includes a detailed error budget which provides important information for the inverse model. Errors associated with the observations in the context of the inverse model include errors in CTM transport and other CTM parameters, the errors in representativeness due to the inability of the model to simulate observed sub-grid scale structure, and instrument noise. We describe a new method of quantifying CTM errors from the mean difference statistics between the simulated and observed CO concentrations, exploiting the high density of observations available from the aircraft mission. Mean bias between the model (with *a priori* emissions) and the observations is assumed to reflect errors in emissions, while the relative variance about this mean bias is assumed to reflect errors in transport. The model transport errors derived in that manner are in the range 20-30%. The representativeness error, estimated from the observed sub-grid variability in the aircraft CO data, is typically 5-10%. Instrument noise ($<$1%) is negligibly small relative to the other sources of error.

Our inverse model analysis implies a 30% increase in Chinese anthropogenic emissions (to 142 Tg CO/yr) of CO relative to the *a priori*. *A posteriori* anthropogenic emissions from other countries are not so different from their *a priori* values. Our best estimate of Asian

anthropogenic emissions is much lowere than previous model studies that used sparse surface observations of CO as constraints [*Kasibhatla et al.*, 2002; *Pétron et al.*, 2002]. We find that *a priori* emissions of CO from biomass burning in Southeast Asia and India are too high, consistent with MOPITT observations during TRACE-P [*Heald et al.*, 2002a] but inconsistent with other TRACE-P studies that used HCN as a tracer for biomass burning [*Li et al.*, 2002; *Heald et al.*, 2002b]. Anthropogenic Chinese sources of HCN may complicate interpretation of CO-HCN correlations [*Singh et al.*, 2002]. Acetonitrile (CH_3CN) or methyl chloride appear to be more robust tracers of biomass burning [*Singh et al.*, 2002; *Blake et al.*, 2002].

Our future work will exploit the correlations of CO with other species to improve the top-down constraints for the inversion of the TRACE-P observations. For example, including CH_3CN in the inverse model analysis should provide valuable constraints on emissions of CO from biomass burning [*Li. et al.*, 2002]. Including CO_2 should help to disaggregate emissions from Korea and Japan whose CO_2/CO emission ratios are very different [*Suntharalingam et al.*, 2003].

Acknowledgments. This work was supported by the NASA Atmospheric Chemistry Modeling and Analysis Program and Global Tropospheric Chemistry Program. We thank Prasad Kasibhatla, Greg Carmichael, Loretta Mickley, and Andrew Fusco for useful discussions.

References

Bergamaschi, P., R. Hein, M. Heimann, and P. J. Crutzen, Inverse modeling of the global CO cycle 1. Inversion of CO mixing ratios, *J. Geophys. Res.*, *105*, 1909–1927, 2000.

Bey, I., et al., Global modeling of tropospheric chemistry with assimilated meteorology: Model description and evaluation, *J. Geophys. Res.*, *106*, 23,073–23,096, 2001a.

Bey, I., D. J. Jacob, J. A. Logan, and R. M. Yantosca, Asian chemical outflow to the Pacific: origins, pathways and budgets, *J. Geophys. Res.*, *106*, 23,097–23,114, 2001b.

Bey, I., D. J. Jacob, R. M. Yantosca, H. Liu, and G. W. Sachse, Quantifying errors in chemical tracer forecasts for aircraft missions, *J. Geophys. Res.*, *submitted*, 2002.

Blake, N. C., et al., NMHCs and halocarbons in Asian continental ouflow during TRACE-P: Comparison to PEM-West B, *J. Geophys. Res.*, *submitted*, 2002.

Bousquet, P., P. Ciasis, P. Peylin, M. Ramonet, and P. Monfray, Inverse modeling of annual atmospheric CO_2 sources and sink: 1. Method and control inversion, *J. Geophys. Res.*, *104*, 26,161–26,178, 1999.

Carmichael, G. R., et al., Evaluating regional emission estimates using TRACE-P observations, *J. Geophys. Res.*, *submitted*, 2002.

Duncan, B. N., J. A. Logan, I. Bey, R. V. Martin, D. J. Jacob, R. M. Yantosca, P. C. Novelli, N. B. Jones, and C. P. Rinsland, Model study of the variability and trends in carbon monoxide (1988-1997) 1. Model formulation, evaluation, and sensitivity, *J. Geophys. Res.*, *submitted*, 2002a.

Duncan, B. N., R. V. Martin, A. C. Staudt, R. Yevich, and J. A. Logan, Seasonal variability of biomass burning emissions constrained by satellite observations, *Accepted J. Geophys. Res.*, 2002b.

Fiore, A. M., D. J. Jacob, I. Bey, R. M. Yantosca, B. D. Field, and J. Wilkinson, Background ozone

over the United States in summer: origin and contribution to pollution episodes, *J. Geophys. Res.*, *107*, doi:10.1029/2001JD000982, 2002.

Heald, C. L., D. J. Jacob, L. Emmons, J. C. Gille, D. J. Westberg, G. W. Sachse, E. V. Browell, M. A. Avery, and S. A. Vay, Transpacific transport and chemical evolution of asian pollution observed from satellite and aircraft, *J. Geophys. Res.*, *submitted*, 2002a.

Heald, C. L., D. J. Jacob, P. I. Palmer, M. J. Evans, G. W. Sachse, H. B. Singh, and D. R. Blake, Biomass burning emission inventory with daily resolution: application to aircraft observations of asian outflow, *J. Geophys. Res.*, *submitted*, 2002b.

Jacob, D. J., et al., The Tranport And Chemical Evolution over the Pacific (TRACE-P) mission: design, execution and overview of results, *J. Geophys. Res.*, *submitted*, 2002.

Kasibhatla, P., A. Arellano, J. A. Logan, P. I. Palmer, and P. Novelli, Top-down estimate of a large source of atmospheric carbon monoxide associated with fuel combustion in Asia, *Geophys. Res. Lett.*, *29*, 2002.

Kiley, C. M., et al., An intercomparison and evaluation of aircraft-derived and simulated co from seven chemical transport models during the TRACE-P experiment, *J. Geophys. Res.*, *submitted*, 2002.

Li., Q., et al., Transatlantic transport of pollution and its effects on surface ozone in Europe and North America, *J. Geophys. Res.*, p. 10.1029/2001JD001422, 2002.

Li, Q., D. J. Jacob, R. M. Yantosca, C. L. Heald, H. B. Singh, M. Koike, Y. Zhao, G. W. Sachse, and D. G. Streets, A global 3-D model evaluation of the atmospheric budgets of HCN and CH_3CN: constraint from aircraft measurements over the western Pacific, *J. Geophys. Res.*, *submitted*, 2002.

Liu, H., D. J. Jacob, I. Bey, R. M. Yantosca, B. N. Duncan, and G. W. Sachse, Transport pathways for

Asian combustion outflow over the Pacific: interannual and seasonal variations, *J. Geophys. Res., submitted*, 2002.

Ma, Y., et al., The characteristics and influence of biomass burning aerosols on fine particle ionic composition measured in Asian outflow during TRACE-P, *J. Geophys. Res., submitted*, 2002.

Martin, R. V., D. J. Jacob, R. M. Yantosca, M. Chin, and P. Ginoux, Global and regional decreases in tropospheric oxidants from photochemical effects of aerosols, *J. Geophys. Res., in press*, 2002.

Novelli, P. C., K. A. Masarie, and P. M. Lang, Distributions and recent changes in carbon monoxide in the troposphere, *J. Geophys. Res.*, *103*, 19,015–19,033, 1998.

Olivier, J. G. J., A. F. Bouwmann, C. W. M. V. der Mass, J. J. M. Berdowski, C. Veldt, J. P. J. Bloos, A. J. J. Visschedijk, and J. L. Haverlag, Description of EDGAR version 2.0: A set of global emission inventories of greenhouse gases and ozone-depleting substances for all anthropogenic and most natural sources on a per country basis and on $1^{\circ} \times 1^{\circ}$ grid, Tech. Rep. 771060002, National Institute of Public Health and the Environment (RIVM) Bilthoven, The Netherlands, 1996.

Palmer, P. I., D. J. Jacob, L. J. Mickley, D. R. Blake, H. E. Fuelberg, and C. M. Kiley, Asian emissions of CH_3CCl_3, Halon-1211, and other halocarbons deduced from aircraft concentration data, *Submitted*, 2003.

Pétron, G., C. Granier, B. Khattatov, J.-F. Lamarque, V. Yudin, J.-F. Müller, and J. Gille, Inverse modeling of carbon monoxide surface emissions using CMDL network observations, *J. Geophys. Res., submitted*, 2002.

Prather, M., and D. Enhalt, Chapter 4: Atmospheric Chemistry and Greenhouse Gases, in "Climate

Change 2001: The Scientific Basis", J. T. Houghton *et al* (ed), Cambridge University Press, 2001.

Prinn, R. G., et al., Evidence for substantial variation of atmospheric hydroxyl radicals in the past two decades, *Science*, *292*, 1882–1888, 2001.

Rodgers, C. D., Retrieval of Atmospheric Temperature and Composition from Remote Measurements of Thermal Radiation, *Reviews of Geophysics and Space Science, 14*, 609–624, 1976.

Sachse, G. W., G. F. Hill, L. O. Wade, and M. G. Perry, Fast-response, high-precision carbon monoxide sensor using a tunable diode laser absorption technique, *J. Geophys. Res.*, 1987.

Singh, H. B., et al., In-situ measurements of HCN and CH_3CN in the Pacific troposphere: sources, sinks, and comparisons with spectroscopic observations, *J. Geophys. Res., submitted*, 2002.

Streets, D. G., et al., An inventory of gaseous and primary aerosol emissions in Asia in the year 2000, *J. Geophys. Res., submitted*, 2002.

Stroppiana, D., S. Pinnoch, and J.-M. Gregoire, The Global Fire Product: daily fire occurrence from April 1992 to December 1993 derived from NOAA AVHRR data, *Int. J. Rem. Sens., 21*, 1279–1288, 2000.

Suntharalingam, P., et al., Constraints of Asian carbon fluxes using CO_2/CO correlation from TRACE-P, *J. Geophys. Res., in preparation*, 2003.

Tang, Y., et al., The influences of biomass burning during TRACE-P experiment identified by the Regional Chemical Transport Model, *J. Geophys. Res., submitted*, 2002.

Yevich, R., and J. A. Logan, An assesment of biofuel use and burning of agricultural waste in the developing world, *Global Biogeochemical Cycles, Accepted*, 2002.

Received _____

Submitted to the *Journal of Geophysical Research*, 2002.

This manuscript was prepared with AGU's LaTeX macros v5, with the extension package 'AGU^{++}' by P. W. Daly, version 1.5b from 1996/10/24.

Tables

Table 1. Annual *a priori* sources of CO (Tg CO yr^{-1}) for the inverse model analysis.

Region	Biofuels[1,2] (**BF**)	Biomass burning[1,2] (**BB**)	Fossil Fuel[1,2] (**FF**)	Methane and biogenic NMVOCs
China (**CH**)	45±32	19±10	64±27	
Korea (**KR**)	4±2	0.3±0.2	5±2	
Japan (**JP**)	2±0.4	0.8±0.4	7±3	
India (**IN**)	29±24	39±20	17±8	
Southeast Asia (**SEA**)	38±35	82±41	16±7	
Rest of World (**RW**)	70±32	340±176	273±60	
TOTAL	188±62	481±176	382±67	1205±301

[1]Sources from BF, BB, and FF include the secondary source of CO from the oxidation of NMVOCs co-emitted with CO.

[2]The magnitude and uncertainty of emission estimates for fuel consumption from East Asia are from *Streets et al.* [2002] (section 3); emissions estimates for fuel consumption in the rest the world are from *Yevich and Logan* [2002] for biofuel and *Duncan et al.* [2002a] for fossil fuel; global emission estimates for biomass burning are from *Duncan et al.* [2002b], with temporal variability over the TRACE-P period from *Heald et al.* [2002b]; and the global source from oxidation of methane and biogenic NMVOCs is as described in the text.

Figures

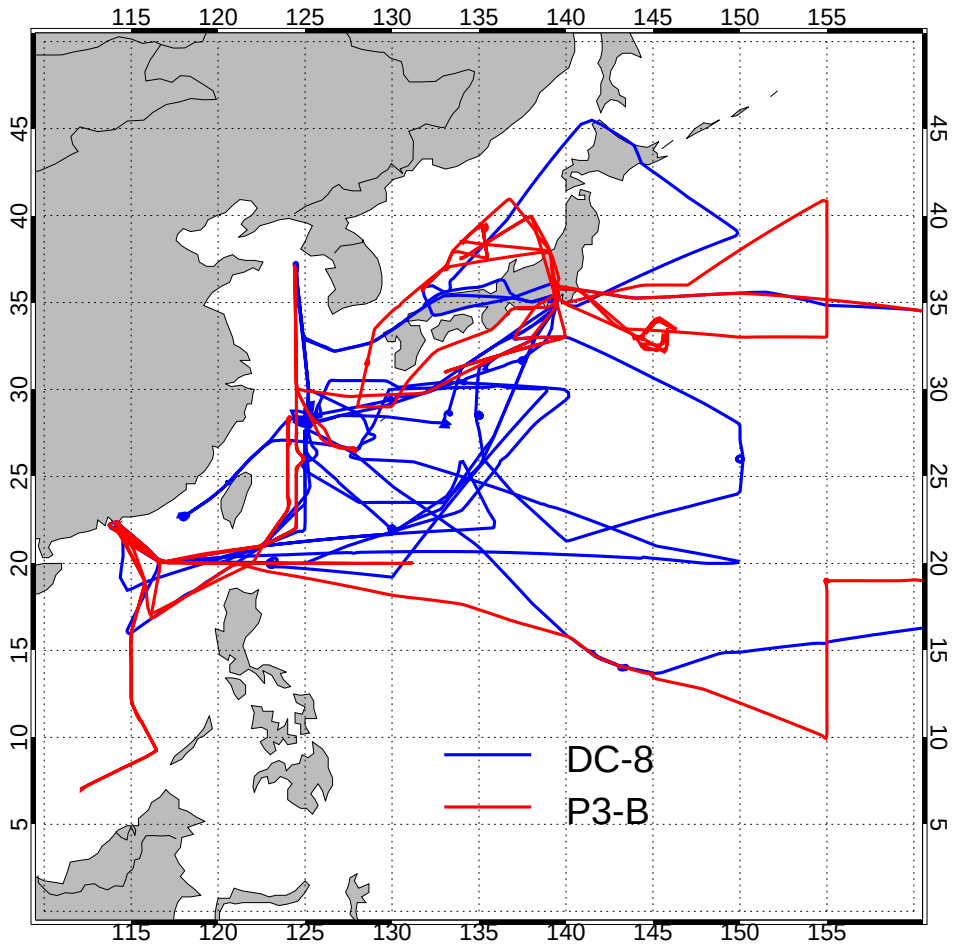

Plate 1. TRACE-P flight tracks for the DC-8 and P3-B aircraft. The inverse model is applied to the ensemble of data west of 150°E which includes 229 hours of CO measurements from the two aircraft, distributed over 28 flights from Feburary 27th to April 3rd, 2001.

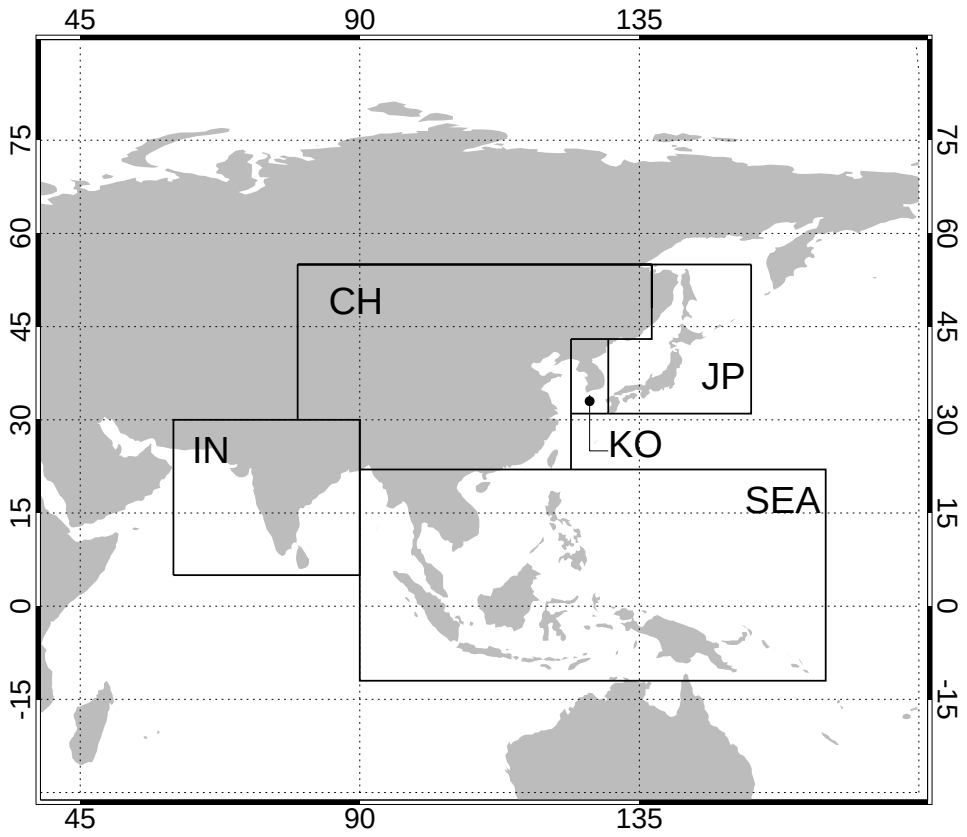

Figure 1. Source regions for tagged CO simulations. See Table 1 for emission estimates.

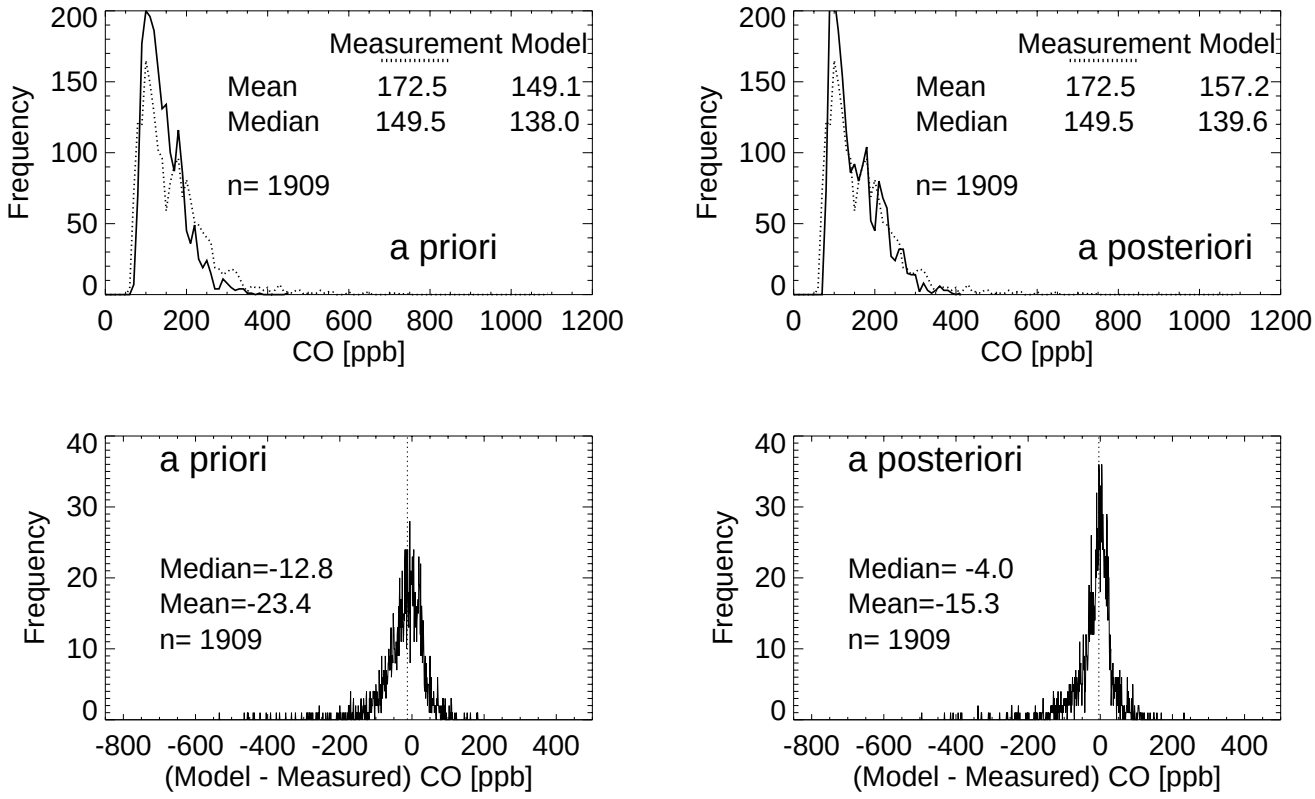

Figure 2. Statistical comparison of simulated and observed CO from TRACE-P, for the model with *a priori* sources (left panels) and *a posteriori* sources (right panels). The observations have been averaged over the $2\times2.5^\circ$ model grid. Data influenced by the stratosphere ($O_3 > 100$ ppb) or away from the western Pacific rim (longitudes $> 150^\circ$E) are excluded from the comparison. Top: frequency distributions of simulated (solid) and observed (dotted) CO. Bottom: frequency distribution of the difference between simulated and observed CO.

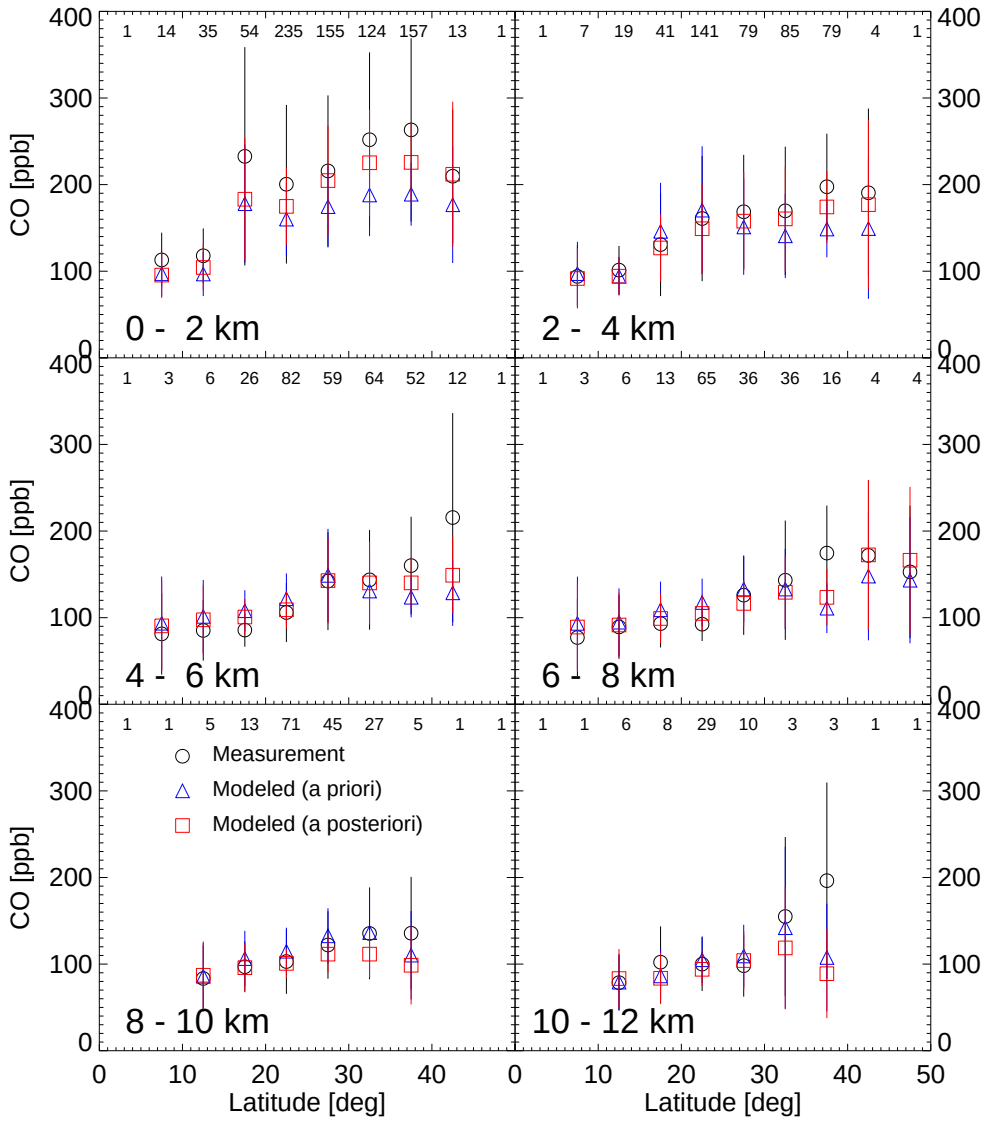

Plate 2. Latitudinal gradients of measured and modeled CO concentrations over the TRACE-P domain on a $2\times2.5^\circ$ grid. Observations (circles) are averaged over the altitude range shown in the figure, and over 5° latitude bins. Vertical bars denote 1-σ values about the mean. The model is sampled along the TRACE-P flight tracks for the flight days, and values are averaged across the same latitude and altitude ranges as the observations. Model values are shown for the simulations with *a priori* (triangles) and *a posteriori* (squares) sources. Data influenced by the stratosphere ($O_3 > 100$ ppb) or away from the western Pacific rim (longitudes $> 150^\circ$E) have been excluded from the comparison. Numbers inset at the top of each panel refer to the number of observations used to compute the mean statistics.

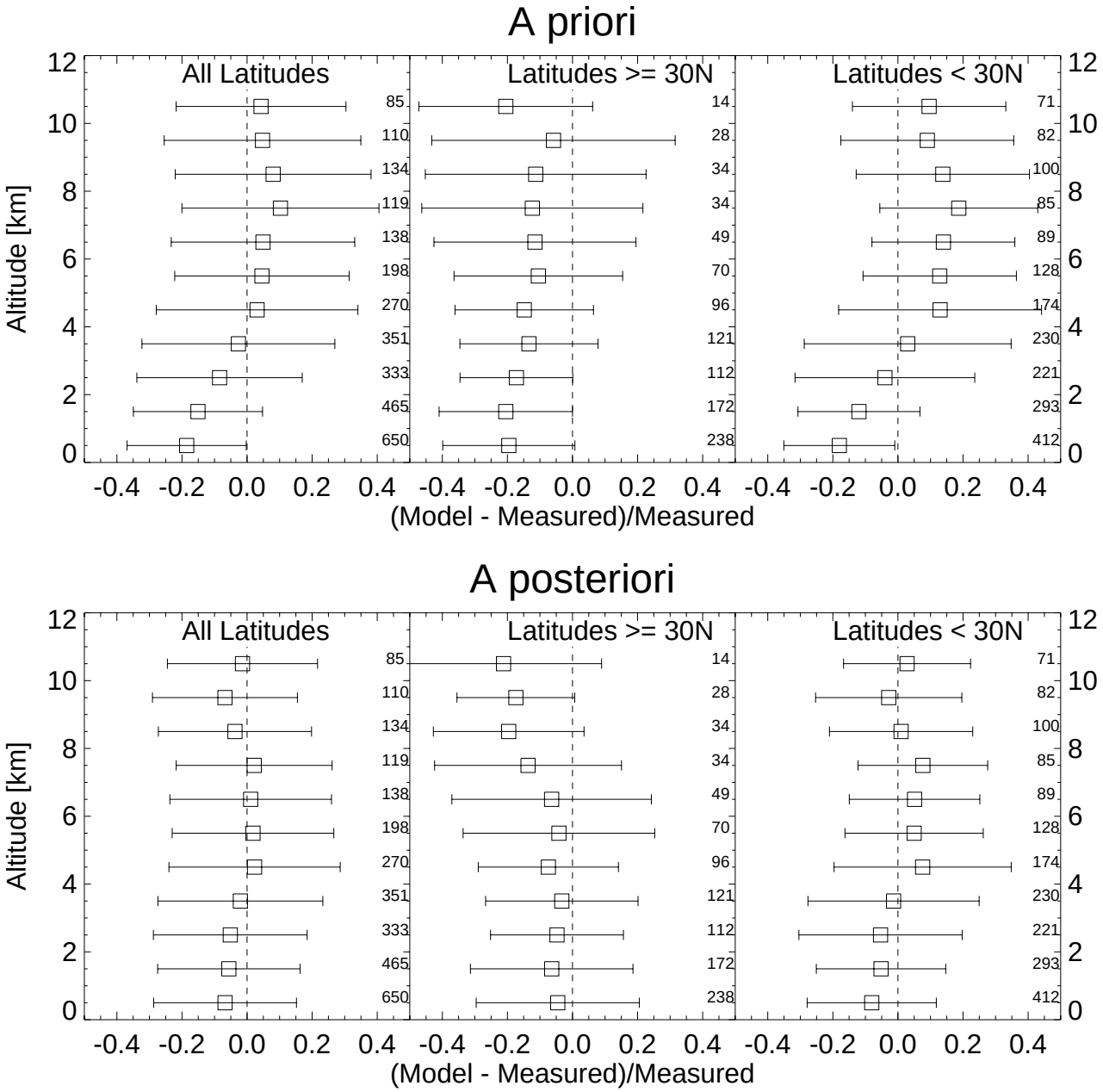

Figure 3. Relative GEOS-CHEM model errors in the simulation of CO during TRACE-P, as a function of altitude for the model *a priori* sources of CO (top) and *a posteriori* sources (bottom). Squares denote the mean bias and horizontal lines denote 1-σ values about the mean. Numbers inset of each panel refer to the number of observations used to compute statistics at each altitude.

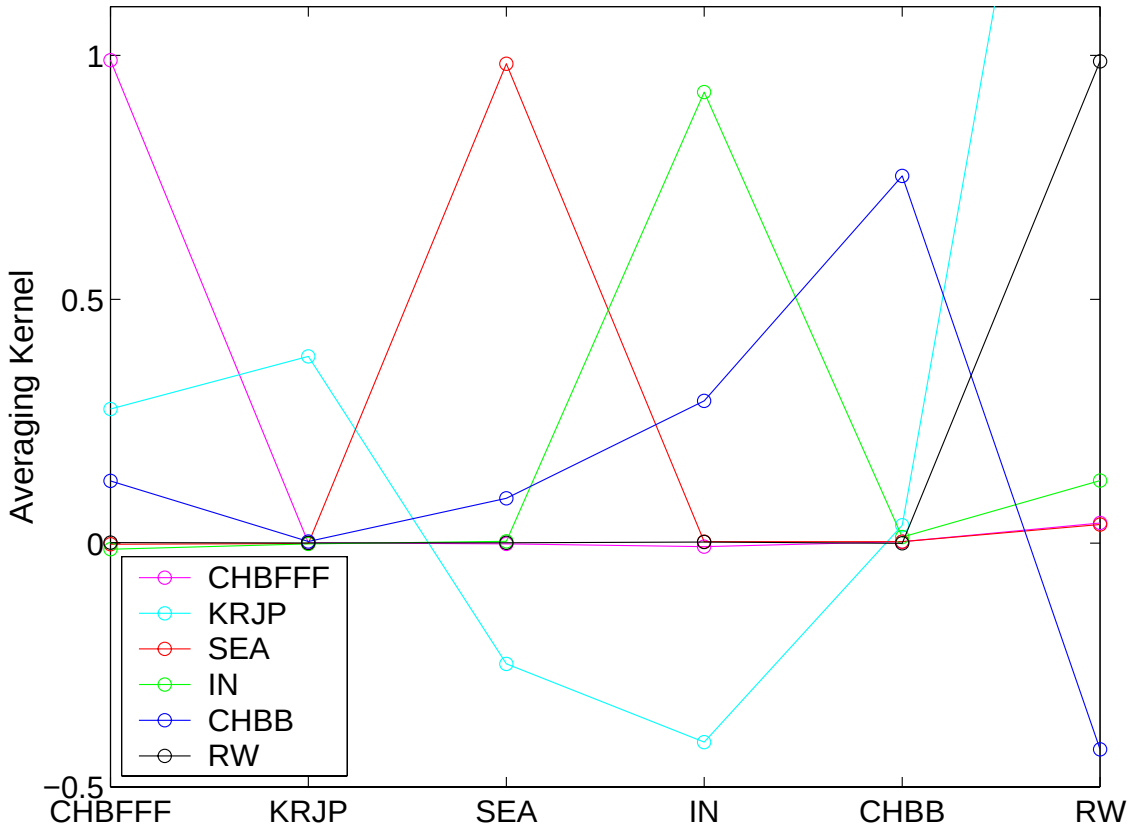

Plate 3. Individual rows of the averaging kernel matrix **A** for the inversion of CO sources with the TRACE-P observing system. Different colors distinguish rows of **A**, listed in the legend, with the corresponding columns indicated on the x-axis. Lines connect the symbols for clarity and do not have any physical significance. The six-element state vector includes sources from Chinese fuel consumption (**CHBFFF**), total emissions from Korea and Japan (**KRJP**), total emissions from Southeast Asia (**SEA**), total emissions from India (**IN**), Chinese biomass burning (**CHBB**), and the rest of the world (**RW**) including the source of CO from biogenic VOCs.

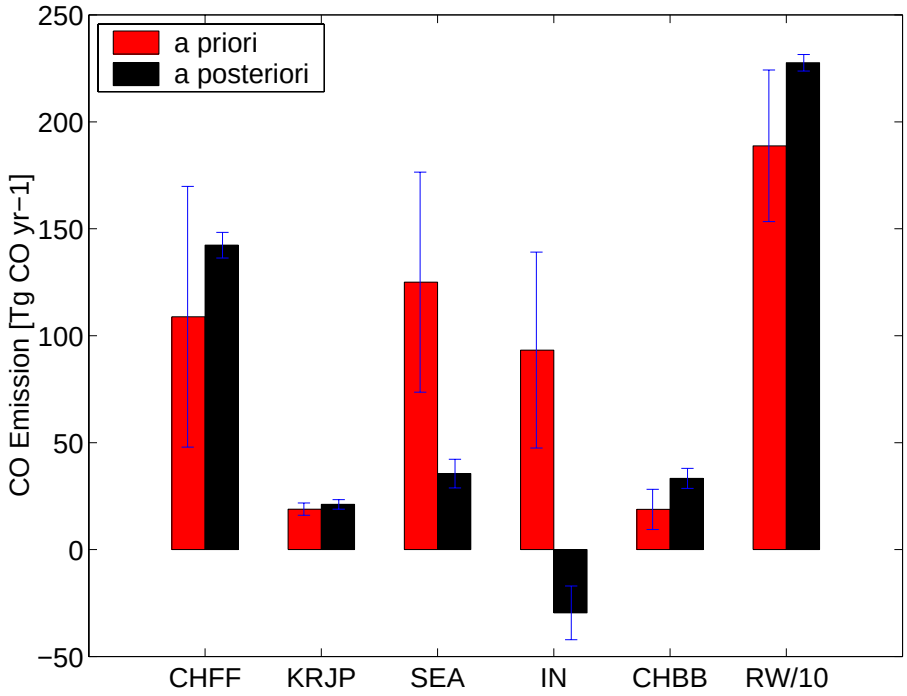

Plate 4. *A posteriori* sources calculated using TRACE-P observations. The error bars represent the 1-σ value about the mean. *A priori* sources are presented alongside for comparison. Elements in the abscissa are as in Plate 3.

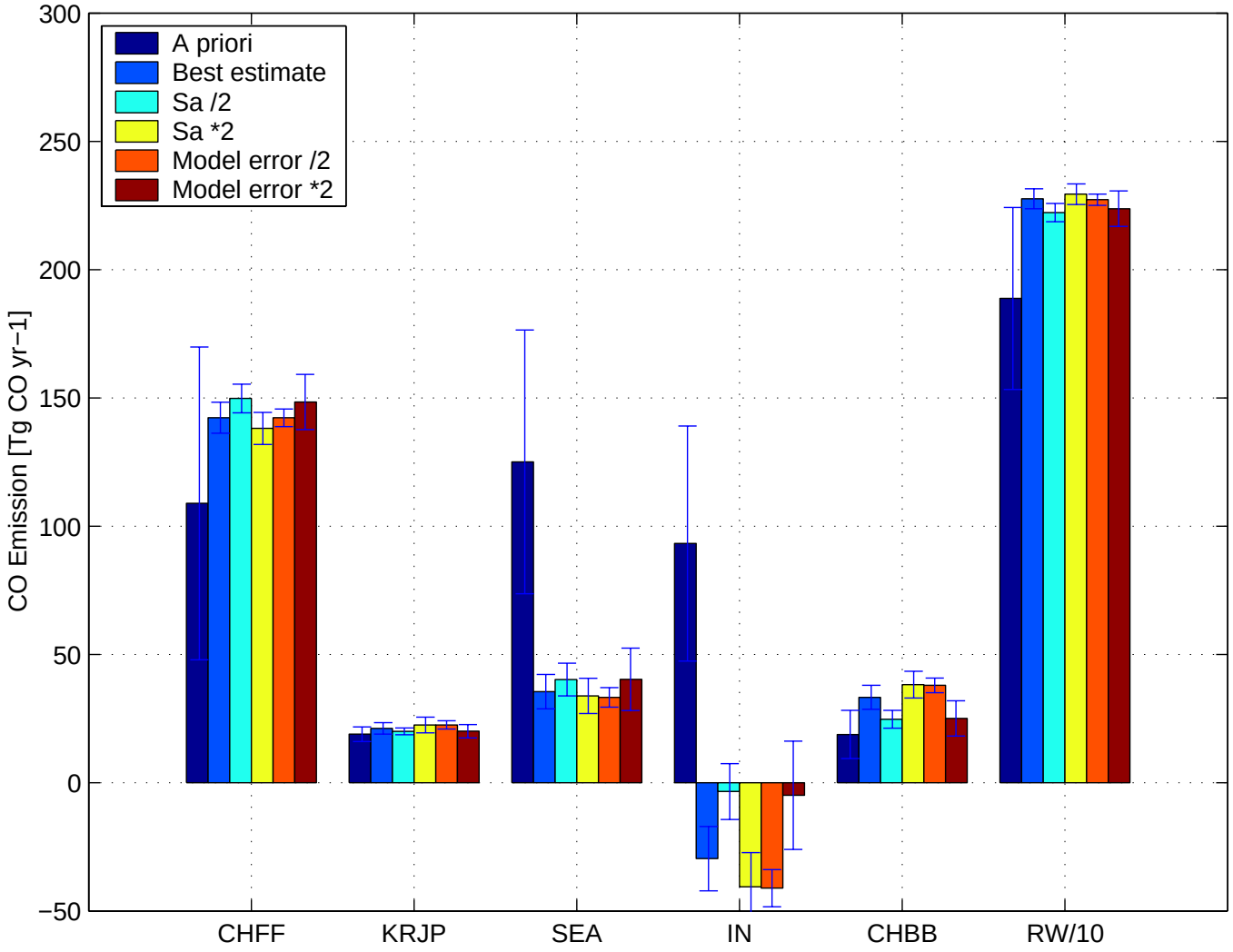

Plate 5. Sensitivity of the calculated *a posteriori* sources to the error estimates in the inverse model. Vertical bars denote 1-σ value from $\hat{\mathbf{S}}$. "Best estimate" shows the *a posteriori* source from the standard inversion (Plate 4). *A posteriori* sources derived from inversions with modified errors on the *a priori* source ($\mathbf{S}_a$) or on the model error are also shown. Elements in the abscissa are as in Plate 3.